Dissociative ionization cross sections of CO_2 at electron impact energy of 5 keV*

Wang En-Liang(王恩亮)†, Shen Zhen-Jie(沈镇捷), Yang Hong-Jiang(阳弘江), Tang Ya-Guo(唐亚国), Shan Xu(单 旭), and Chen Xiang-Jun(陈向军)

Hefei National Laboratory for Physical Sciences at Microscale and Department of Modern Physics, University of Science and Technology of China, Hefei 230026, China
Synergetic Innovation Center of Quantum Information and Quantum Physics, University of Science and Technology of China, Hefei 230026, China

(Received 9 April 2014; revised manuscript received 13 May 2014; published online 17 September 2014)

The dissociative ionization of CO_2 induced by 5 keV electrons in two-body and three-body dissociative channels of CO_2^{2+} and CO_2^{3+} is identified by the ion–ion coincidence- method using a momentum imaging spectrometer. The partial ionization cross sections (PICSs) of different ionic fragments are measured and the results generally agree with the calculations made by a semi-empirical approach. Furthermore, the PICSs of the dissociative channels are also obtained by carefully considering the detection efficiency of the micro-channel plates and the total transmission efficiency of the time of flight system.

Keywords: electron collision, partial ionization cross section, dissociative ionization cross section, momentum imaging

PACS: 34.80.Gs, 34.80.Ht **DOI:** 10.1088/1674-1056/23/11/113404

1. Introduction

The electron impact ionization of molecules is of fundamental importance in atmospheric physics,[1] plasma processes,[2,3] mass spectrometry,[4,5] etc. In the studies of these related fields, the reliable data of the total or partial ionization cross sections (PICSs), which correspond to the production of all ions or a specific kind of ion, are needed. The data for CO_2 are of special interest because CO_2 plays an essential role in the planetary atmosphere and interstellar space.[6,7] In spite of the great importance, the data of the ionization cross sections for CO_2 are still quite scarce. Most of the previous experimental studies on the electron impact PICSs of CO_2 were limited to the low-energy regime from the threshold to 1 keV.[8–16] Only recently, were the PICSs of CO_2 reported at an electron impact energy of 10–26 keV by Bhatt *et al.*[17,18]

In recent years, the electron collision dynamics, as well as the associated molecular dissociation dynamics, have captured continuous interest.[19,20] It is very interesting to clarify the decay pathways of the multiply ionized molecules, which is the main topic of most of the related works. However, it would also be meaningful to precisely determine the cross sections for certain dissociation channels of the molecular ions. Conventionally, a time of flight (TOF) spectrometer is adapted to measure the PICSs. In order to obtain the PICSs for different dissociative ionization channels, a multi-coincidence technique must be used to detect the ionic fragments in coincidence. With the help of this technique, Bhatt *et al.* have measured the PICSs of CO_2 for different dissociative channels of the molecular ions at an impact energy of 12 keV.[18] Interestingly, there is a large gap in the 1–10 keV region where almost no experimental data are available. In the present work, channel-resolved PICSs of CO_2 at the electron impact energy of 5 keV are reported using a newly developed ion momentum imaging spectrometer in our laboratory.

2. Experiments and data analysis

The experiment was carried out using an electron impact ion imaging spectrometer. The experimental setup has been described in detail elsewhere.[21] Briefly, a pulsed electron beam from a thermal cathode electron gun is injected into the reaction center to collide with the gas target. After the collision, a pulsed extraction field is applied to extract the ions. A Wiley–Mclaren type TOF mass spectrometer[22] is employed to collect the ions with 4π solid angle. The lengths of the acceleration and the drift regions are 50 mm and 100 mm, respectively. At the end of the TOF system, a multi-hit time and position sensitive detector (RoentDek DLD 120) is used to detect the TOFs and the positions of the ions. The position resolution of the detector is better than 0.5 mm. The time resolution of the data acquire system is calibrated to be better than 50 ps.[21] By using the pulsed electron beam, we are able to eliminate the influence of the extraction field to the electron beam, which perplexed Sharma *et al.*[23] and Singh *et al.*[24] in their instruments. Furthermore, using the pulsed electron

*Project supported by the National Basic Research Program of China (Grant No. 2010CB923301), the National Natural Science Foundation of China (Grant Nos. 11327404, 10979007, and 10734040), and the Fundamental Research Funds for the Central Universities, China.

†Corresponding author. E-mail: elwang@ustc.edu.cn

© 2014 Chinese Physical Society and IOP Publishing Ltd

beam will also significantly reduce the background and, hence, reduce the noise-to-signal ratio. In the present work, the target gas beam system has been modified to improve the momentum resolution. A capillary is mounted on a manipulator and is then inserted in the center of the pushing and pulling electrodes. The capillary is kept at the ground potential. With the help of the manipulator, the capillary is adjusted to the position of the ground potential of the extracted field to eliminate the distortions of the extracted field. The inner diameter, the outer diameter, and the length of the capillary are 0.1 mm, 0.3 mm, and 50 mm, respectively. The high ratio of length to inner diameter of the capillary enables a collimated gas beam. The image size of CO_2^+ is less than 2 mm×2 mm. The momentum resolution of CO_2^+ is about 15 a.u., which is approximate to the thermal momentum spread at room temperature.

In the present work, the energy of the electron beam is fixed at 5.0 keV. The pulse width and the repetition frequencies of the electron beam are 10 ns and 15 kHz, respectively. The beam current is kept at 1 pA. The extraction field is 50 V/cm. The background vacuum is better than 5.0×10^{-6} Pa, and the pressure rises up to 1.0×10^{-4} Pa when the gas is loaded. The purity of the CO_2 sample gas is better than 99.995%.

For the TOF spectrum of a single ionic fragment, the true count rate $N(X^+)$ for a specific type of detected ion X^+ is

$$N(X^+)=\frac{C(X^+)-R}{D(X^+)}, \tag{1}$$

where $C(X^+)$ is the detected count rate, R is the background count rate, and $D(X^+)$ is the efficiency factor, which is the product of the detection efficiency of the micro-channel plates (MCPs) and the transmission efficiency of the TOF system. In this work, for each type of ion of interest, the detected count rate $C(X^+)$ is larger than the background count rate R by at least two orders of magnitude. Consequently, the background count rate can be omitted. In the following analysis, the factor $D(X^+)$ is considered to be a constant for all ions; that is, $D(X^+)=D$.

The following four predominant dissociative channels are analysed for the double or triple ionization of CO_2 in this work:

$$CO_2^{2+*}\rightarrow O^+ + CO^+, \tag{2}$$
$$CO_2^{2+*}\rightarrow C + O^+ + O^+, \tag{3}$$
$$CO_2^{2+*}\rightarrow C^+ + O^+ + O, \tag{4}$$
$$CO_2^{3+}\rightarrow C^+ + O^+ + O^+. \tag{5}$$

For channels (2)–(4), the two associated ions X^+ and Y^+ must be detected in coincidence. The relationship between the true coincidence count rate $N(X^+ + Y^+)$ and the detected coincidence count rate $C(X^+ + Y^+)$ for these channels can be expressed as

$$N(X^+ + Y^+)=\frac{C(X^+ + Y^+)}{D^2}. \tag{6}$$

For the three-body Coulomb explosion channel (5), the true count rate of the triple coincidence is

$$N(C^+ + O^+ + O^+)=\frac{C(C^+ + O^+ + O^+)}{D^3}, \tag{7}$$

where $C(C^+ + O^+ + O^+)$ is the detected coincidence count rate. In order to obtain the cross sections of channels (2)–(5), the efficiency factor D must be assessed using an appropriate method. In the study of Bhatt *et al.*,[17,18] the efficiency factor D was taken to be the product of the open area ratio (55%) of the MCPs and the estimated transmission efficiency (30%–40%) of the meshes of the TOF system. However, the absolute detection efficiency of the MCPs is actually less than the open area ratio. As investigated in the work of Brehm *et al.*,[25] the maximum absolute detection efficiency was determined to be less than 45% for the MCPs with an open area ratio of 57%. In the present work, the detection efficiency of the MCPs and the transmission efficiency of the meshes are determined in more detail. On the one hand, the voltage applied on the front surface of the MCPs is kept at −2.1 kV, which assures the ion impact energy of about 2.1 keV. The detection efficiency of the MCPs is taken to be the same value of Ar^+, which is 30%±2%, as measured by Brehm *et al.*[25] at the same impact energy. They also show that the detection efficiencies of different ions have almost the same value at the same impact energy. Therefore, the same value of 30%±2% is applied to the other ions in this work. On the other hand, a series of four meshes, M1, M2, M3, and M4, is introduced in the present TOF system. M1 and M2 are single-layered meshes with transmission efficiencies of 90% and 80%, respectively. M3 is mounted at the end of the drift tube, and M4 is installed between the drift tube and the MCPs. Both M3 and M4 are double layered to prevent field penetration. Although the shielding effect is significantly improved by the double-layered meshes, the transmission efficiency is almost the same as the single-layered one (80%) for the thin mesh.[26,27] The total transmission efficiency of the TOF system is 46.1%. As a result, the efficiency factor D is determined to be 13.8%.

3. Results and discussion

The TOF spectrum of the single ionic fragment is shown in Fig. 1. The most intense peak originates from the single ionization of CO_2. The mass resolution can be estimated from the width of the CO_2^+ peak. The full width at half maximum (FWHM) of the CO_2^+ peak is 16 ns, while the TOF center is at 6381 ns. This gives a mass resolution $m/\Delta m = T/2\Delta T = 200$, which is much better than that in the previous work[21] and which is comparable to the result of Sharma *et al.*[23] The peak of CO_2^{2+} originates from the double ionization of CO_2. The other peaks, CO^+, O^+, and C^+, originate from the dissociative

ionizations. The C^{2+} and O^{2+} are not presented in this work due to the poor data statistics. The peak at 5460 ns, which can be ascribed to O_2^+, which is the parent ion of O_2, may be due to the background impurity. Fortunately, there is no inference of O_2^+ with the ions from the interested dissociative channels in this work.

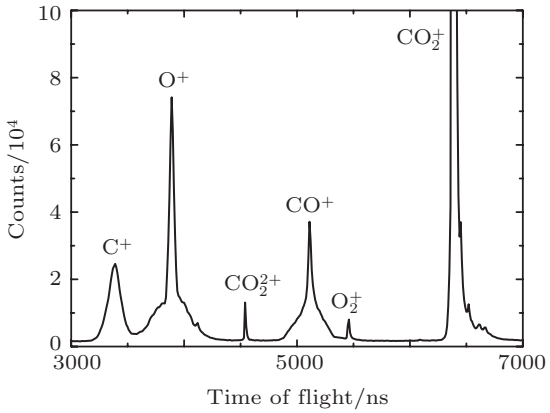


Fig. 1. TOF spectrum of ionic fragments arising from the electron impact ionization of CO_2.

In the present experiment, only the relative cross sections are obtained. The data are put on the absolute scale by normalizing the PICS for CO_2^+ to the calculated ones using a semi-empirical approach (SEA),[28] which is based on the Born–Bethe and Møller formula.[28,29] The PICS of SEA can be expressed as

$$Q_i(E) = \int\int Q_i(E,W,\theta) 2\pi \sin\theta \,\mathrm{d}\theta \,\mathrm{d}W, \tag{8}$$

with

$$\begin{aligned} &Q_i(E,W,\theta) \\ &= \left\{ \frac{a_0^2 R^2}{E} \int\limits_{\boldsymbol{K}\to 0} \frac{E-W}{E-I_i} \frac{1}{W} \mathrm{d}f_i(W,\boldsymbol{K},\theta) \ln[1+C_i(E-I_i)] \right. \\ &\left. + \frac{E-I_i}{E(\varepsilon_0^3+\varepsilon^3)} S_i \left[\varepsilon - \frac{\varepsilon^2}{E-\varepsilon} + \frac{\varepsilon^2}{(E-\varepsilon)^2} \right] \right\} \sin\theta, \end{aligned} \tag{9}$$

where W, a_0, R, $\boldsymbol{K}$, S, θ, and $\mathrm{d}f_i$ are the electron energy loss, the first Bohr radius, Rydberg's constant, the momentum transfer, the number of ionizable electrons, the scattering angle, and the differential generalized oscillator strength, respectively. Here $\mathrm{d}f_i(W,\boldsymbol{K},\theta)$ in the optical limit ($\boldsymbol{K}\to 0$) has been used. The SEA requires the input data of the optical oscillator strengths and converts the photoionization cross section data to PICS.[28] The results of the SEA are adopted here because, on the one hand, the *ab-initio* calculations of the PICSs for the molecular system are not available at present.[28] On the other hand, the SEA has been successfully applied to calculate the total ionization cross sections and the PICSs for different molecules,[28,30] which agree well with the experimental results.

The same normalizing factor of CO_2^+ is then applied to the other ionic fragments and the dissociation channels. So we have

$$\mathrm{PICS}(X^+) = \mathrm{PICS}(CO_2^+) \frac{C(X^+)}{C(CO_2^+)}, \tag{10}$$

$$\mathrm{PICS}(X^+ + Y^+) = \mathrm{PICS}(CO_2^+) \frac{C(X^+ + Y^+)}{C(CO_2^+)D}, \tag{11}$$

$$\mathrm{PICS}(C^+ + O^+ + O^+) = \mathrm{PICS}(CO_2^+) \frac{C(C^+ + O^+ + O^+)}{C(CO_2^+)D^2}. \tag{12}$$

The PICSs of CO_2 for the productions of CO_2^+, CO^+, CO_2^{2+}, O^+, and C^+ at the electron impact energy of 5 keV together with the results of Bhatt *et al.* at 10 keV,[17] 12 keV,[18] and those of Straub *et al.*[14] at lower impact energies are shown in Table 1. To compare the experiments with the calculations, the measured PICSs together with the results of the SEA are plotted in Fig. 2. As can be seen in the figure, the present results of PICSs for CO_2^+ (shown by squares) and CO_2^{2+} (stars) at 5 keV and the data of Straub *et al.* at lower energies generally agree with the theoretical calculations, while the results of Bhatt *et al.* at 10 keV and 12 keV seem much larger if we extrapolate the theoretical curves to the relevant energies. As for the PICSs of the fragments O^+ (circles), C^+ (diamonds), and CO^+ (triangles), the consistency between the experiments and the calculations becomes poorer. Our result for C^+ agrees quite well with the calculation, while the one for CO^+ is lower and the one for O^+ is larger than the theoretical predictions. All of the PICSs for these three ionic fragments obtained by Bhatt *et al.* at 10 keV and 12 keV again are much higher than the theoretical predication. Interestingly, there are

Table 1. Partial ionization cross sections (in units of 10^{-18} cm^2) for ionic fragments of CO_2 at the electron impact energy from 0.1 keV to 12 keV. Errors (in percentage) are given in brackets.

	Present 5.0 keV	12 keV[a)]	10 keV[b)]	1.0 keV[c)]	0.5 keV[c)]	0.1 keV[c)]
CO_2^+	24 (9.4)	13.9 (8)	18.5	89.0	138	237
CO^+	4.0 (9.4)	1.95 (8)	2.8	10.5	18.3	41.0
O^+	6.8 (9.4)	3.55 (8)	4.4	21.2	37.1	67.5
C^+	3.3 (9.4)	1.38 (8)	1.4	9.79	17.3	32.7
CO_2^{2+}	0.44 (9.4)	0.17 (9)	0.248	0.735	1.45	2.80

[a)]Ref. [18], [b)]Ref. [17], [c)]Ref. [14].

intersections between the theoretical curves for the three fragments at the impact energies of 4–5 keV, which is contradictory with our experiments and those of Bhatt *et al*. In this respect, further precise measurements and calculations are required.

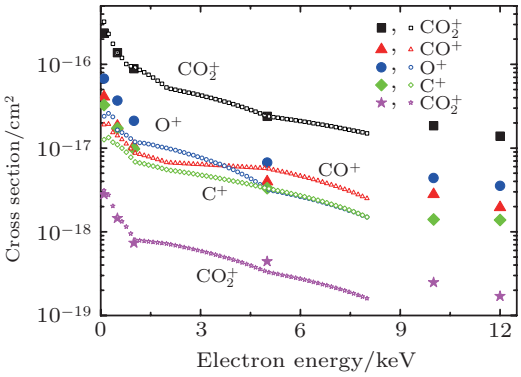


Fig. 2. (color online) Partial ionization cross sections for different ionic fragments from the multiple ionized CO_2 induced by electrons at different impact energies. The solid and open symbols correspond to experimental and theoretical results, respectively. The experimental results at electron energy 0.1–1.0 keV, 10 keV, and 12 keV are from Refs. [14], [17], and [18], respectively. The theoretical results are from Ref. [28].

In order to identify the dissociative channels (2)–(5), the ion–ion coincidence method[31] is introduced. The coincidence can be achieved by drawing the two-dimensional TOF spectrum of the detected ions. The ions originating from one dissociative channel are scattered along the diagonal lines. The ion–ion coincidence spectra are shown in Fig. 3. The coincidence islands $a1$ and $a2$ in Fig. 3(a) correspond to channels (2) and (3), respectively. Both channels (4) and (5) contribute to the coincidence island $a3$ in Fig. 3(a). Channel (5) can further be identified by using the triple coincidence method, which has been described in detail in Ref. [21]. Briefly, the coincidence island between C^+ and the first O^+ (island $a3$ in Fig. 3(a)), together with the coincidence island between C^+ and the second O^+ (island $b1$ in Fig. 3(b)), can jointly determine channel (5). The coincidence count rate of dissociative channel (4) can thus be expressed as

$$\begin{aligned} N(C^+ + O^+ + O) &= N(C^+ + O^+) - N(C^+ + O^+ + O^+) \\ &= \frac{C_{a3}}{D^2} - \frac{C_{b1}}{D^3}, \end{aligned} \tag{13}$$

where $N(C^+ + O^+)$ is the true coincidence count rate of island $a3$, and C_{a3} and C_{b1} are the detected coincidence count rates of islands a3 and $b1$, respectively.

The PICSs for dissociative channels (2)–(5) are presented in Table 2. The results of Bhatt *et al*.[18] at 12 keV are also summarized in this table. For channels (2) and (3), which contribute solely to islands $a1$ and $a2$, respectively, the measured PICSs of this work at 5 keV are about 2–3 times larger compared to those of Bhatt *et al*. at 12 keV. The present PICS of channel (5), which leads to three final fragment ions, is about 3.4 times larger than that of Bhatt *et al*., where a factor of D^2 should be taken into account in obtaining the absolute value of the PICS, as shown in Eq. (12). Then, according to Eq. (13), the PICS of channel (4) can be deduced, which is 2.4 times larger than the result of Bhatt *et al*. at 12 keV. As mentioned above, D is determined to be 13.8% in this work, while it was estimated to be about 24%, which is simply the product of the open area ratio of the MCP and the estimated transmission efficiency of the TOF system in the work of Bhatt *et al*. The likely overestimation of D in their work will lead to the lower estimations of the PICSs. If 13.8% is used instead, the relevant PICSs should be approximately 1.7 times higher for the two-body dissociative channels (2)–(4) and $1.7^2 \sim 2.9$ times higher for the three-body dissociative channel (5). Considering the decrease of the PICSs with the increase of the impact energy, Bhatt *et al*. may also have overestimated the PICSs for all four dissociative channels. Actually, if we investigate the branching ratios, both works obtain similar values for these channels.

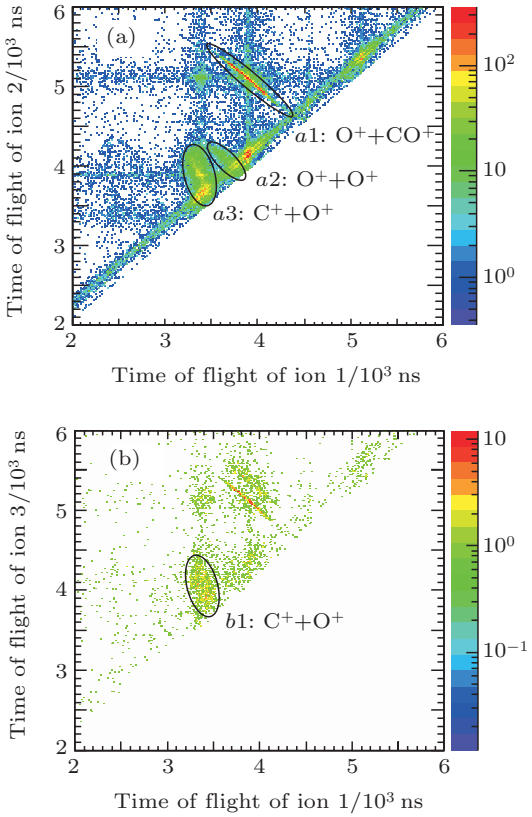


Fig. 3. (color online) Ion–ion coincidence spectrum of the ionic fragments from the multiple ionized CO_2. (a) The first versus the second ions. The coincidence islands $a1$ and $a2$ correspond to dissociative channels (2) and (3), respectively. Both dissociative channels (4) and (5) contribute to coincidence island $a3$. (b) The first versus the third ions. Coincidence island $b1$ corresponds to dissociative channel (5). The signals along the diagonal in the two spectra are caused by the miss-trigger of the same single time signal of the first hit ion due to its oscillating tail.

Table 2. Partial ionization cross sections (in units of 10^{-18} cm^2) and branching ratios (%) for the major dissociative channels of CO_2^{2+} and CO_2^{3+}. Errors (in percentage) are given in brackets.

Dissociative channel	Present 5 keV		12 keV[a)]	
	PICSs	Branching ratios	PICSs	Branching ratios
O^++CO^+	0.74 (9.4)	37.8	0.3730 (8)	45.8
C+O^++O^+	0.35 (9.4)	18.2	0.1060 (8)	13.0
C^++O^++O	0.69 (9.4)	35.3	0.2850 (9)	35.1
C^++O^++O^+	0.17 (9.4)	8.7	0.0500 (10)	6.1

[a)] Ref. [18].

4. Conclusion

The investigation on the dissociative ionization of CO_2 induced by 5 keV electrons is carried out using a momentum imaging system combined with a multi-hit time and position sensitive detector. The PICSs for ions CO_2^+, CO^+, CO_2^{2+}, O^+, and C^+ are obtained and put on the absolute scale by normalizing the PICS for parent ion CO_2^+ to the calculated values by a semi-empirical approach.[28] The PICSs for CO_2^+, CO_2^{2+}, and C^+ agree quite well with the calculation results, while those for CO^+ and O^+ are, respectively, lower and larger than the theoretical predictions. The PICSs for the three major dissociative channels of doubly ionized CO_2, as well as the PICS for the Coulomb explosion channel of triply ionized CO_2, are also obtained. The 5 keV results are 2–4 times larger than the reported data of Bhatt *et al.*[18] at 12 keV. Considering the possible overestimation of the efficiency factor D, as well as the decrease of the PICSs with the increase of the impact energy, Bhatt *et al.* may have overestimated the PICSs for the dissociative channels.

References

[1] Hugh R M 1989 *Physics and Chemistry of the Upper Atmosphere* (Cambridge: Cambridge University Press)
[2] Jiang J, Dong C Z, Xie L Y, Wang J G, Yan J and Stephan F 2007 *Chin. Phys. Lett.* **24** 691
[3] Zhang S B, Wang J G and Janev R K 2010 *Phys. Rev. Lett.* **104** 023203
[4] Dörner R, Mergel V, Jagutzki O, Spielberger L, Ullrich J, Moshammer R and Schmidt-Böcking H 2000 *Phys. Rep.* **330** 95
[5] Ullrich J, Moshammer R, Dorn A, Dörner R, Schmidt L P H and Schmidt-Böcking H 2003 *Rep. Prog. Phys.* **66** 1463
[6] Shimonishi T, Onaka T, Kato D, Sakon I, Ita Y, Kawamura A and Kaneda H 2008 *Astrophys. J. Lett.* **686** L99
[7] Thissen R, Witasse O, Dutuit O, Wedlund C S, Gronoff G and Lilensten J 2011 *Phys. Chem. Chem. Phys.* **13** 18264
[8] Donald R and Paula E G 1965 *J. Chem. Phys.* **43** 1464
[9] Adamczyk B, Boerboom A J H and Łukasiewicz M 1972 *Int. J. Mass Spectrom.* **9** 407
[10] Crowe A and McConkey J W 1974 *J. Phys. B* **7** 349
[11] Märk T D and Hille E 1978 *J. Chem. Phys.* **69** 2492
[12] Orient O J and Strivastava S K 1987 *J. Phys. B* **20** 3923
[13] Krishnakumar E 1990 *Int. J. Mass Spectrom.* **97** 283
[14] Straub H C, Lindsay B G, Smith K A and Stebbings R F 1996 *J. Chem. Phys.* **105** 4015
[15] Tian C and Vidal C R 1998 *J. Chem. Phys.* **108** 927
[16] Tian C and Vidal C R 1998 *Phys. Rev. A* **58** 3783
[17] Bhatt P, Singh R, Yadav N and Shanker R 2010 *Phys. Rev. A* **82** 044702
[18] Bhatt P, Singh R, Yadav N and Shanker R 2011 *Phys. Rev. A* **84** 042701
[19] Ren X, Pflüger T, Xu S, Colgan J, Pindzola M S, Senftleben A, Ullrich J and Dorn A 2012 *Phys. Rev. Lett.* **109** 123202
[20] Xu S, Ma X, Ren X, Senftleben A, Pflüger T, Dorn A and Ullrich J 2011 *Phys. Rev. A* **83** 052702
[21] Wang E L, Shan X, Shi Y F, Tang Y G and Chen X J 2013 *Rev. Sci. Instrum.* **84** 123110
[22] Wiley W C and McLaren I H 1955 *Rev. Sci. Instrum.* **26** 1150
[23] Sharma V and Bapat B 2006 *Eur. Phys. J. D* **37** 223
[24] Singh R, Bhatt P, Yadav N and Shanker R 2011 *Meas. Sci. Technol.* **22** 055901
[25] Brehm B, Grosser J, Ruscheinski T and Zimmer M 1995 *Meas. Sci. Technol.* **6** 953
[26] Williams D L, Read F H and Bowring N J 1995 *Nucl. Instrum. Meth. A* **363** 120
[27] Lu Z G and Tian J B 2008 *Appl. Opt.* **47** 5519
[28] Pal S 1999 *Chem. Phys. Lett.* **308** 428
[29] Jain D K and Khare S P 1976 *J. Phys. B* **9** 1429
[30] Kim Y K and Rudd M E 1994 *Phys. Rev. A* **50** 3954
[31] Frasinski L J, Codling K and Hatherly P A 1989 *Science* **246** 1029